8. Summary and Conclusions

In this work a new type of core-multishell architecture *via* straight forward three-step synthesis was developed. As precursor, cheap, commercially available building blocks were used. These systems can act as universal supramoleculary aggregated hosts to encapsulate various types of guest molecules such as polar (congo red, vitamin B_6, rose bengal) and nonpolar (nimodipine, β-carotene, nile red) organic molecules or metal ions. The solubility of these polymers in a broad range of solvents permit the transport of guest molecules into polar or nonpolar environments independent of the guests' polarity and solubility (Scheme 21). This is in contrast to already existent systems (micelles, polymeric micelles, micelle-like core-shell architectures) which can either transport nonpolar molecules into aqueous environment, or transfer polar molecules into a hydrophobic media. Since the encapsulation of polar and nonpolar molecules in liposomes based systems is only possible in water, they cannot be applied in organic solvents. Therefore, core-multishell architectures, with their universal transport behavior, can be considered as "chemical chameleons".

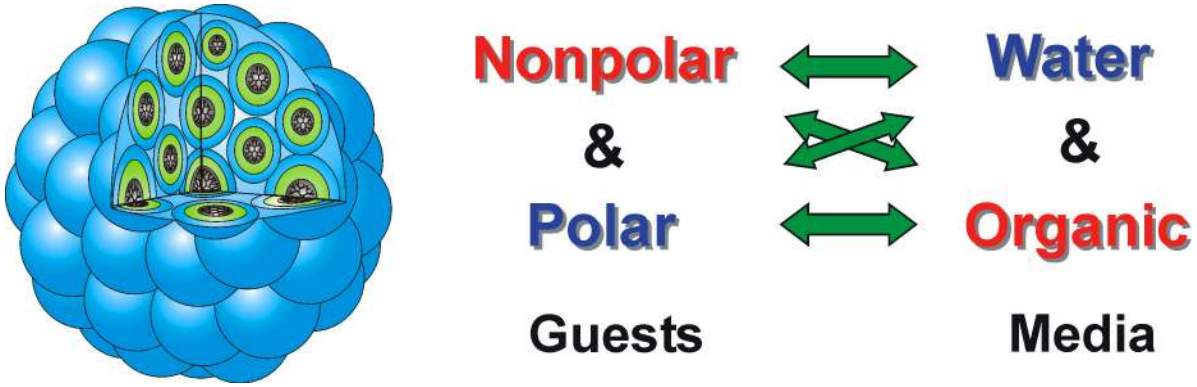

Scheme 21. Universal transport abilities of core-multishell architectures as supramolecular aggregates.

To understand the role of the individual domains (core, inner shell, outer shell) of these multishell architectures for the transport of guest molecules each individual part was varied. As a core two hyperbranched polyethyleneimines with different molecular weight (M_n = 3600 g mol^{-1}, PD = 1.4; M_n = 10500 g mol^{-1}, PD = 2.0), hyperbranched polyglycerols polymer (M_n = 10000 g mol^{-1}, PD = 1.7), and PAMAM[G5] dendrimer (M_n = 14204 g mol^{-1}) were chosen. These hyperbranched or dendritic cores were functionalized with linear amphiphilic building blocks formed by alkyl diacids (C_0, C_6, C_{12}, or C_{18}) connected to monomethyl poly(ethylene glycol) ethers (mPEG with 6, 10, 14, or 22 glycol units on average) with different degrees of functionalization (Figure 70).

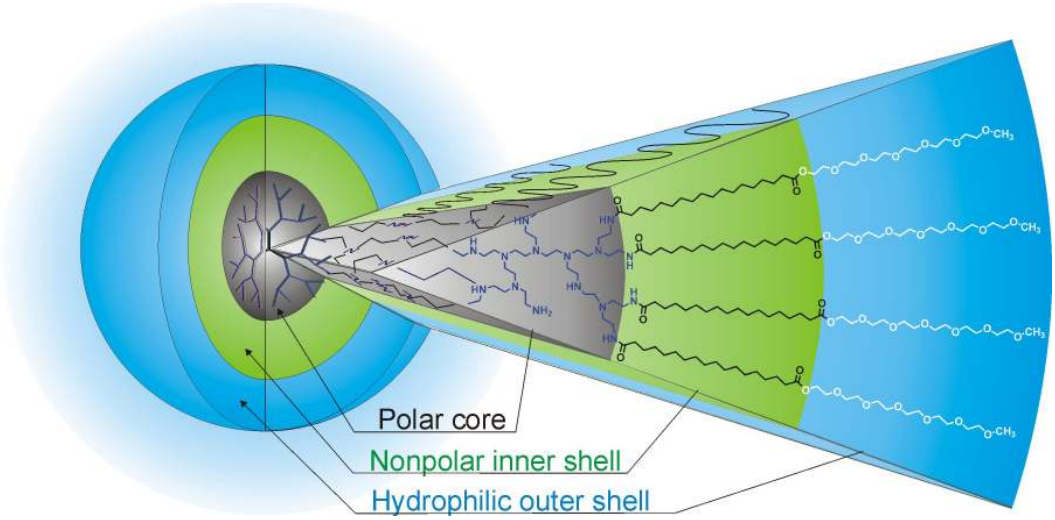

Figure 70. Schematic picture of core-multishell architectures.

Encapsulation experiments revealed that modifications of every domain quantitatively influence the transport capacities of polymers. Increase of the PEI core size improves TC for polar and nonpolar molecules. However, differences in molecular mass of polymers only cause relative transport capacities to increase for polar molecules, while polymers with a smaller core are more suitable for hydrophobic guests. Further optimization of the TC for polar or nonpolar compounds can be achieved by modifying the degree of the core functionalization. With increased shell density (higher degree of functionalization) the encapsulation efficiency for hydrophobic guests also increase while the transport capacity for polar guests significantly decreases at the same time. Change of the core type from hyperbranched PEI into hyperbranched PG results in decreasing (typically by a factor of 2) transport capacities and relative transport capacities for polar guest molecules and increasing TC and TC_{rel} (by a factor of 1.5 to 2.0) for nonpolar ones. Nanotransporters with PAMAM core show comparable transport capacities to the polymers with PEI core. The size of the biocompatible mPEG shell had a limited, but still important, effect on the transport capacity. With an increased chain length from ~6 to ~14 glycol units an increase of the TC for all polymers (independent of the core size and degree of functionalization) by a factor of ~1.5 has been observed. In contrast to the quantitative changes caused by modifications of core and outer shell, the presence of the inner, hydrophobic domain is essential for encapsulation abilities of core-multishell architectures (qualitative influence). This influence was crucial for both polar and nonpolar guest molecules. Introduction of the aliphatic C_{18} chain allowed encapsulation of nonpolar molecules and increased the transport capacity of congo red approximately 77 times in comparison to the polymer without inner shell (Figure 71).

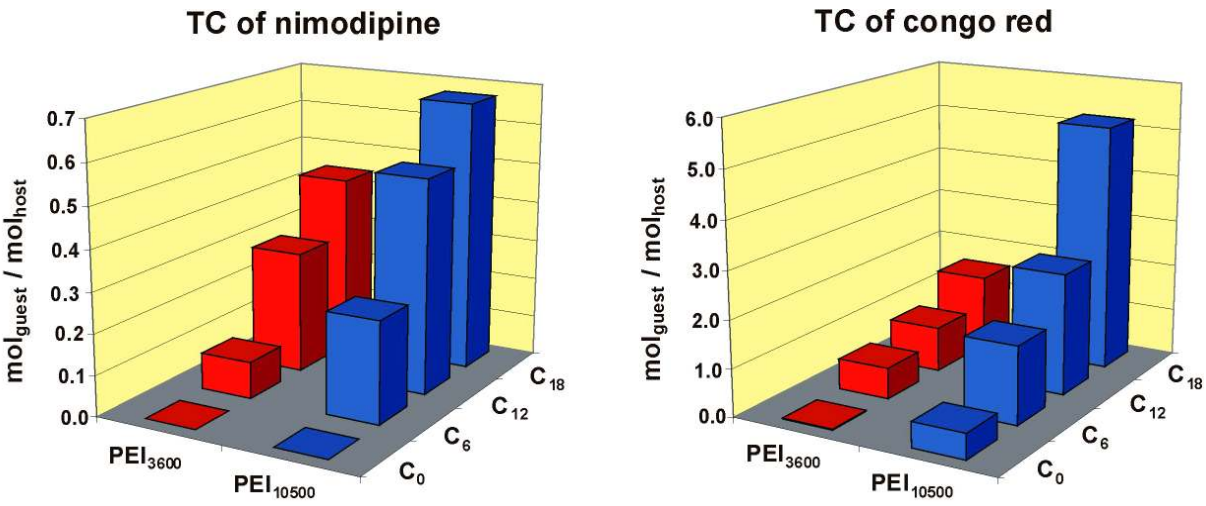

Figure 71. Influence of the inner shell length on the transport capacity of the $PEI_x(C_ymPEG_6)_{0.9}$ (x = 3600, 10500; y = 0, 6, 12, 18) polymers for nimodipine (left) and congo red (right). No transport of nimodipine and congo red could be detected in absence of nanocarriers. For clarity reasons the error bars are not shown, and they are in the range of 10 %.

Additionally, the influence of nonstructural factors, such as polymer concentration, guest molecule concentration, and time of encapsulation, on the transport capacity of nanotransporters has been established.

Experiments performed for the dilution series revealed a nonlinear transport capacity behavior for a linear change of polymer concentration with three distinguishable regions (concentration ranges). At low polymer concentrations (usually below 0.05 g l^{-1}) no transport of guest molecules into the solution was observed. With increasing polymer concentration, at the threshold point, located typically in the range of 0.05 to 0.20 g l^{-1} (independently from the molecular mass of the polymer), a rapid increase of the transport capacity to its maximal value appeared. This initial growth of TC is usually followed with a sharp drop of the encapsulation efficiency, which is caused by a further increase of the concentration in the range from 0.20 to approximately 1.00 g l^{-1}. Above this concentration slow stabilization of transport capacity value can be observed (Figure 72). This behavior was confirmed experimentally for all synthesized core-multishell architectures independent of the type of encapsulated guest molecule and is similar to the behavior observed for amphiphilic molecules (low molecular mass surfactants or diblock copolymers). The existence of threshold concentration in polymers encapsulation profile suggests aggregation phenomena of nanotransporters.

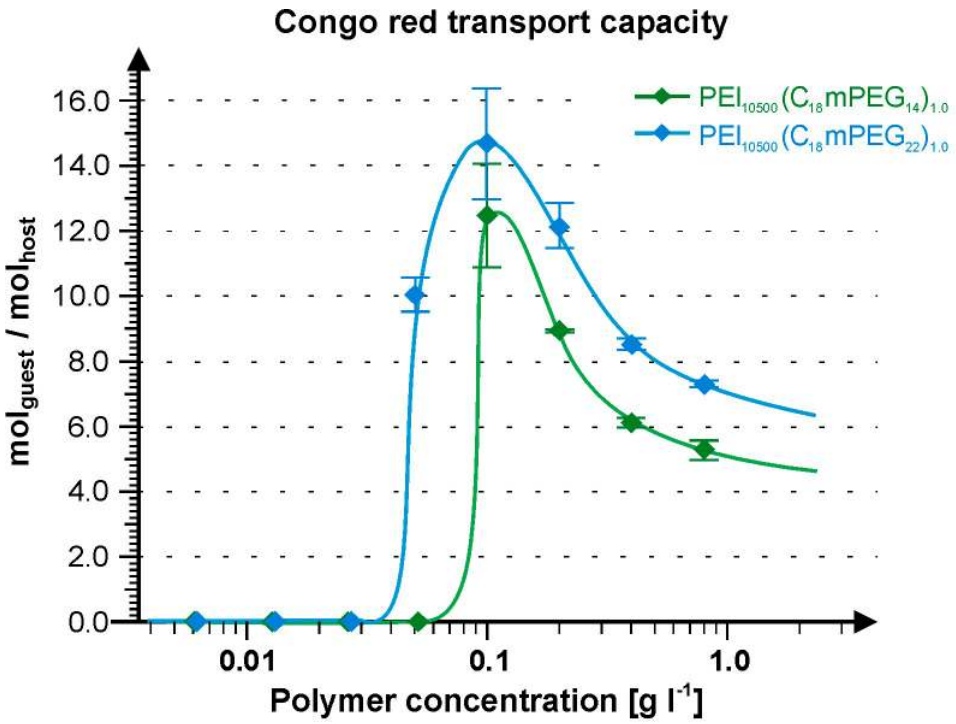

Figure 72. Influence of polymer concentration on the transport capacity for congo red with polymers $PEI_{10500}(C_{18}mPEG_{14})_{1.0}$ and $PEI_{10500}(C_{18}mPEG_{22})_{1.0}$ as examples of nonlinear encapsulation-polymer concentration dependency.

To better understand the underlying principles of transport abilities of core-multishell architectures, the aggregation phenomenon was investigated by three independent techniques: surface tension measurement, dynamic light scattering (DLS), and CyroTEM. Results of these experiments were described in the second part of this thesis.

The aggregation properties of the nanotransporters were analyzed over a wide concentration range from 0.002 to 4.0 g l^{-1} by surface tension measurement in a pendant drop apparatus. The surface tension decreased linearly with the logarithm of the polymer concentration as suggested by the Gibbs adsorption isotherm which implies that core-multishell architectures do behave like amphiphilic compounds. In addition, the surface activity critical aggregation concentrations (CACs – characteristic concentration above which surface tension remains almost constant) for various polymers, including influence of structural composition of the polymer on CAC value, were determined. In analogy to the critical micelle concentration (CMC) of surfactants it was assumed that an aggregation process between individual nanotransporters (“unimers”) takes place in the solution above the CAC. This is in good agreement with the previously observed nonlinear transport capacity behavior as a function of polymer concentration. This suggests that core-multishell architectures do not act as unimolecular carrier systems. Instead, the measurement indicates that supramolecular aggregates are responsible for their transport ability.

To confirm this hypothesis DLS and CryoTEM measurements were performed. Obtained results revealed coexistence of two types of species in the polymeric solution above CAC: smaller with a diameter in the range of 4 to 8 nm (unimers) and bigger with a diameter of 30 to 50 nm (aggregates) (Figure 73 a and d). Size of the "unimers" was also confirmed by negative staining TEM and AFM and results in the diameter of 7 to 9 nm for a single polymeric molecule. Molecular modelling of the unimolecular polymer, $PEI_{3600}(C_{18}mPEG_6)_{0.7}$, in a periodic water box gave a typical diameter of approximately 6 nm, which is in good agreement with the experimental value. Upon encapsulation of guest molecules a drastic change was observed in the size of the supramolecular aggregates. It is surprising that the size change does not depend on the polarity of the solvent and the guest molecules, but rather on the geometry of the latter. By encapsulation of linear molecules (congo red, β-carotene) the particle size increase from 30 to 50 nm to a diameter of approximately 120 to 150 nm in both solvents, water and chloroform (Figure 73 c and f). For the more globular (compact) molecules (nimodipine, vitamin B_6) the effect was opposite and gave assemblies of approximately 20 to 30 nm in both solvents (Figure 73 b and e). This observation may be a result of the fact that these molecules are preferentially located in the interfacial region and behave as a cosurfactants that reduce the interfacial tension and thus prevent the formation of larger aggregates. This change results also in a reduction of the CAC values for polymers with encapsulated compact molecules. In contrast, linear guest molecules might act as noncovalent linkers between the assemblies' constituents because of their extended geometry. Increasing the aggregate size also result in an increase of the CAC values for polymers with linear guest molecules. The direct structural analyses of supramolecular assemblies by CryoTEM revealed a noticeably granular fine structure of the aggregates. The ultrastructural features are fundamentally different from the CryoTEM images of liposomes and micelles, thus suggesting that the aggregates are indeed formed by a large number (up to 20000) of elementary unimolecular species.

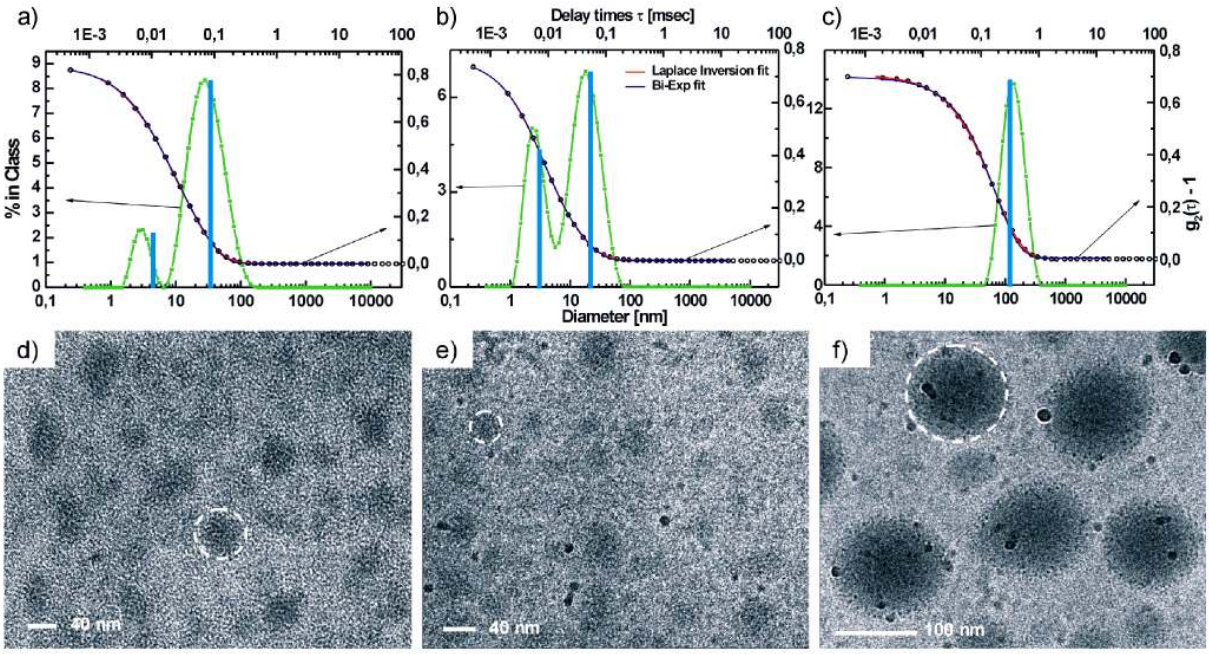

Figure 73. The size of the core-shell architectures, $PEI_{3600}(C_{18}mPEG_6)_{0.7}$, and its aggregates were determined by DLS (a–c) and by CryoTEM (d–f) measurements. For the pure polymer (a) diameters of aggregates were determined by DLS to 34.9 nm (with use of Laplace Inversion) or 34.6 nm (Bi Exponential). The size of polymer aggregates with Nimodipine (b) were found to be 21.9 nm or 23.2 nm. For β-Carotene-polymer aggregates (c) diameters were determined to 144 nm or 121 nm. In addition to the aggregates, the "unimers" have been observed by DLS and the diameters were determined to be ~ 5 nm (a,b). Because of the large dimensions of the β-Carotene-polymer aggregates a detection of unimers was not possible in this case. All results from DLS were confirmed by CryoTEM measurements (c-f). The size of the unimers were determined to be ~5 nm. Aggregate diameters for pure multishell nanocarriers (d) were determined in a range of 30 - 50 nm. After encapsulation of Nimodipine (e) the size changed to diameters of 20 - 30 nm. Encapsulation of β-Carotene (f) increased the size of aggregates to 120 - 150 nm. The concentration of all samples analyzed by CryoTEM and DLS was 1.0 g L^{-1} of polymer in pure water (6 x 10^{-5} M).

Localization of the encapsulated guest molecules in the aggregate structure was performed with the environment-sensitive dye – nile red. Analysis of the UV/Vis absorbance spectra of encapsulated dye as a function of the time of the uptake process, revealed two different nanoenvironments around the guest molecules. This corresponds to the different sites of dye encapsulation.

It was hypothesized that the guest molecule encapsulation by the nanotransporters is based on a two-step process. In the first step dye/drug molecule is encapsulated inside the intermolecular cavities created by mPEG chain network on the surface and at the interface between the polymers in the aggregates. The intermolecular encapsulation process is very fast and the progress can be observed in minutes. In the second step, with the continuation of the uptake (process), encapsulated guests migrate slowly from intermolecular spaces into

the inner (intramolecular) cavities located inside the polymer structure. The intramolecular cavities are not directly reachable in the guest molecules encapsulation process and therefore intermolecular encapsulation (thus aggregation of the polymers) is necessary.

Localization of the guest molecules in the intermolecular cavities was confirmed by AFM measurements. High-quality images of the core-multishell architectures on the HOPG revealed the presence of the encapsulated compounds between the polymers and no intramolecular encapsulation was confirmed by the AFM technique.

In the last part of this thesis antibacterial and fungicidal properties of core-multishell architectures with encapsulated silver(I) ions were investigated. Experiments performed on the *E. coli* culture revealed a minimum of 100 times higher antibacterial activity of the nanotransporters with encapsulated silver ions than the pure silver nitrate solution at the same concentration of the Ag^+. Water solution of polymer at the concentration of 5×10^{-7} M with 15 encapsulated silver (I) ions per host destroyed all bacteria in 10 minutes after addition of the solution on the test plate. More than 90% of the bacteria were destroyed after 1 minute. The fungicidal properties tested with the culture of *A. niger* revealed the absolute inhibition of the fungus growth at the polymer/silver(I) complex concentration of 5×10^{-5} M. Partial growth inhibition was already visible for concentration range of 10^{-7} to 10^{-6} M.

Core-multishell architectures are new and very promising materials for host-guest chemistry. These nanotransporters are fundamentally different in their structure and transport behavior compared to the simple detergent micelles and unimolecular carrier systems reported previously in the literature. The universal encapsulation properties in combination with very good solubility of polymers in broad spectrum of solvents permits the application of this system without further optimization as a versatile tool in various fields. This new core-multishell architecture can be used to transport and/or stabilize the different guest molecules such as drug, dyes, toxic compounds, metal nanoparticles and ions, and fluorescent markers and therefore can find a multiple applications in medicine, pharmaceutical and cosmetics industry, as well as catalysis.